A&A 384, 343–349 (2002)
DOI: 10.1051/0004-6361:20011835

Astronomy & Astrophysics

A comparison of ion irradiation and UV photolysis of CH_4 and CH_3OH

G. A. Baratta, G. Leto, and M. E. Palumbo

Osservatorio Astrofisico di Catania, via S. Sofia 78, 95123 Catania, Italy

Received 4 October 2001 / Accepted 20 December 2001

Abstract. We have studied by infrared absorption spectroscopy the effects induced by fast ions (30 keV) and Lyman-α photons (10.2 eV) on some molecular ices at low temperature (10–20 K). It is well known that in both cases the physical and chemical properties of the ices are modified. However while the energy released by ions depends mainly on their energy and on the target species, the effects induced by photons also depend on the optical properties of the sample. Here we show that the effects of ion irradiation and UV photolysis are comparable on fresh ices (i.e. at low doses) but are increasingly different as processing is continued (i.e. at high doses).

Key words. astrochemistry – molecular processes – methods: laboratory – techniques: spectroscopic – ISM: molecules

1. Introduction

Solid objects in space (interstellar grains, comets, interplanetary dust particles), are continuously exposed to energetic processes such as cosmic ray and UV photon irradiation. Fast ions passing through a molecular solid release energy to the target material. As a consequence many molecular bonds are broken along the ion-track and, in a very short time (one picosec or less), the molecular fragments recombine giving rise to a rearrangement of the chemical structure. Hence, in addition to the alteration of the chemical and lattice structure of the target material, new molecular species (not present before irradiation) are formed. In the case of UV irradiation, the energy is released to the target material through single photo-dissociations, photo-excitations or ionization events per incoming photon. Also in this case new molecular species are formed.

The effects induced by fast ions and UV photons on solids of astrophysical interest have been separately studied in different laboratories for many years (e.g., Hagen et al. 1979; Brown et al. 1982; Moore et al. 1983; Strazzulla et al. 1983; Allamandola et al. 1988; Baratta et al. 1991; Westley et al. 1995; Gerakines et al. 1996; Strazzulla et al. 2001; Moore et al. 2001). It is well known that both processes induce chemical (e.g., Moore et al. 1983; Gerakines et al. 1996) and structural (e.g., Baratta et al. 1991; Moore & Hudson 1992; Baratta & Leto in preparation) modifications of the ice samples. Recently the effects induced by Lyman-α photons and 0.8 MeV H^+ in a H_2O:CO_2 ice mixture have been compared in the same experimental apparatus (Gerakines et al. 2000). Furthermore, Cottin et al. (2001) have presented the analysis of two organic residues formed after UV photolysis or ion irradiation of the same ice mixtures in the same experimental set-up.

Recently, we have added a Lyman-α microwave powered lamp to our experimental apparatus, which for many years has been used to perform ion irradiation experiments. Now this gives us the capability to study (by using in situ Infrared and Raman spectroscopy) the effects induced in frozen gases and solids by fast ions and UV photons. This can be done: (a) comparing the results of separate experiments; (b) switching from one energy source to the other during the same experiment; (c) irradiating the sample simultaneously with ions and UV photons. Examples of cases (a) and (b) are given here.

In this paper we present the experimental set-up, the new calibration procedures and some results of the comparison between ion and UV irradiation of molecular ices.

2. Experimental set-up

The experimental results reported in the next sections have been obtained using in situ infrared (IR) spectroscopy. A schematic view of the experimental apparatus is reported in Fig. 1.

Send offprint requests to: M. E. Palumbo,
e-mail: mepalumbo@alpha4.ct.astro.it

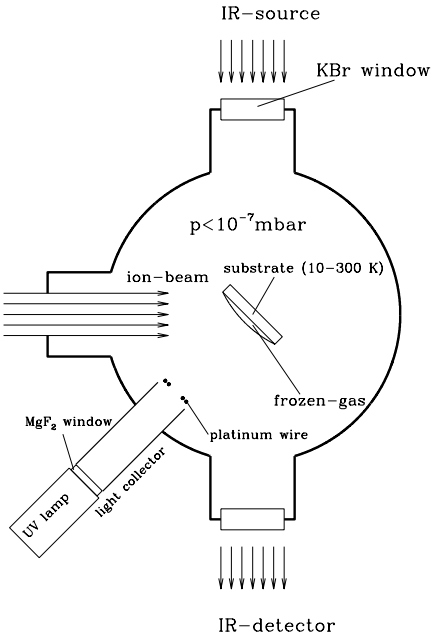

Fig. 1. Schematic view of the experimental apparatus used for in situ IR spectroscopy of ion and UV irradiated frozen gases.

In situ IR spectroscopy is performed in a stainless steel vacuum chamber facing an FTIR spectrometer (Bruker Equinox 55). Inside the vacuum chamber, in which pressure is kept below 10^{-7} mbar, an IR transparent substrate (crystalline silicon) is placed in thermal contact with a cold finger which temperature can be varied between 10 K and 300 K. The vacuum chamber is interfaced with an ion implanter (30 kV; Danfysik) from which ions with energy up to 30 keV (60 keV for double ionizations) can be obtained. The ion beam produce a 2×2 cm^2 spot on the targets and current in the range of 100 nA cm^{-2} to a few μA cm^{-2}.

A hydrogen microwave discharge resonance lamp (Opthos Instruments) is interfaced with the vacuum chamber through an MgF_2 window; from this lamp mainly 10.2 eV photons are obtained. An aluminium light collector is placed at the end of the lamp in order to increase the number of UV photons that reaches the sample. A light detector, placed at the end of the aluminium light collector, is used to measure the UV flux during photolysis. The detector is a platinum wire which gives a current, by the photoelectric effect, proportional to the UV flux. The wire detector has been calibrated using the procedure described in Sect. 3.1.

A needle valve is used to admit pre-prepared gases (or mixtures) into the chamber, where they freeze on the substrate. A He-Ne laser can be used to monitor the thickness of the ice film during accretion; this is achieved by looking at the interference pattern (intensity versus time) given by the laser beam reflected at an angle of 45° both by the vacuum-film and film-substrate interfaces (see Baratta & Palumbo 1998 for further details on the technique used to measure the thickness).

The substrate holder is mounted at an angle of 45° both with the ion beam and with the IR beam and it is orthogonal to the UV beam, so that spectra can be easily taken in situ, even during irradiation with ions and UV photons, without tilting the sample. For this purpose the IR spectrometer is positioned (by a moveable optical bench) such that the IR beam is transmitted, through a hole in the sample holder, by the substrate. In addition to unpolarized transmission spectra at an incidence angle of 45°, spectra with the electric vector parallel (P polarized) and perpendicular (S polarized) to the plane of incidence can be taken. The plane of incidence is the plane of the paper in Fig. 1; this plane contains P polarized light while the plane of S polarization is perpendicular to the paper. The polarization of the incident radiation can be changed rotating a polarizer placed in the path of the infrared beam (Baratta & Palumbo 1998). As shown by Baratta et al. (2000) spectra taken at oblique incidence in S polarization are equivalent to unpolarized spectra at normal incidence.

3. Calibration procedures

3.1. UV lamp wire detector

Following the procedure described by Gerakines et al. (2000) we started calibrating the UV lamp from the conversion of O_2 in O_3 after photolysis of pure O_2. In particular, we have deposited on the cold substrate ($T = 12.5$ K) in the vacuum chamber a sample of O_2, $\sim$1 μm thick. Infrared transmission spectra of the O_2 ice have been taken after photolysis. Due to the lack of data for solid O_3, we have assumed the gas-phase values for both the integrated absorption strength of the O_3 stretching mode at 1030 cm^{-1} ($A = 1.4 \times 10^{-17}$ cm molecule^{-1}; Smith et al. 1985) and the O_3 quantum yield (1.92[1]; Groth 1937) and we have measured first the number of O_3 molecules formed after photolysis, then the number of photons cm^{-2} absorbed by the sample and hence we have estimated the number of photons cm^{-2} impinging on the icy sample. This latter estimate is based on the assumption that 10% of incident photons are reflected or scattered. The amount of reflected light ($\sim$5%) has been deduced in the case of water ice from the optical constants given by Warren (1984).

However the flux of the UV lamp is not stable and can vary also during each experiment. For that reason, we have placed a light detector at the end of the aluminium light collector in order to measure the UV flux during photolysis. The light detector is a platinum wire which has been calibrated with the same procedure used to calibrate the lamp. Thus the number of photons cm^{-2} impinging on the icy sample is correlated to the current value (μA), given by the photoelectric effect, at the platinum wire. The integration over time of the current value is proportional to the integrated flux of the UV lamp. The calibration constant of the wire, given by the ratio between the photon fluence (photons cm^{-2}) measured on the sample and the

[1] This quantum yield value has been measured, using a Xenon lamp, at 1470 Å and 1295 Å (Groth 1937).

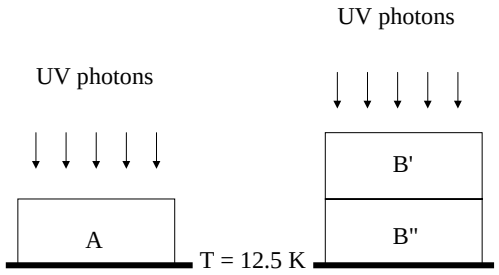

Fig. 2. Schematic of the experiments done to measure the absorption coefficient of Lyman-α photons in molecular ices.

wire current, integrated over the time of photolysis, has been verified to be constant within the whole range of flux provided by the lamp ($10^{13} - 5 \times 10^{14}$ photons cm^{-2} s^{-1}). The presence of the calibrated platinum wire allows us to monitor the UV flux throughout the experiment and to modify the flux during the experiment still having a reliable estimate of the fluence.

3.2. Absorption coefficient

In order to compare the effects that are induced by fast ions and UV photons, the irradiation doses (energy released to the target molecules i.e. eV molecule^{-1}) must be derived. Although doses are normally given for the fast ion irradiation case, up to now this has rarely been done for UV photon irradiation experiments of astrophysically relevant ices. This lack is partially due to the difficulty in evaluating the fraction of UV photons that are effectively absorbed by the ice during photolysis. This quantity indeed depends on the optical constants (n and k) of the irradiated ice that are not known in the majority of cases; furthermore the optical constants of the sample change during UV photolysis. Then the fraction of UV photons effectively absorbed by a particular photolyzed ice for given fluences, has been evaluated by comparing the effects obtained in two different photolysis experiments with the ice samples of different thickness (see Fig. 2).

In particular, for the same ice species, we have considered two samples A and B ($B = B' + B''$ and $B' = B''$), with thickness of B twice that of A, and we have repeated the photolysis experiment on both samples taking IR spectra after the same fluences of UV processing. In first approximation (when reflection and interference effects are neglected), the transmittance $T_{B''}$ of the B'' portion of B is given by the relation: $T_{B''} = T_B/T_A = T_B/T_{B'}$ (in fact A and B', having the same thickness, absorbed the same number of UV photons). The B'' film portion is then equivalent to the A film at a lower UV fluence and the ratio between these fluences can be determined by looking at the corresponding IR spectra. This gives the fraction of UV photons absorbed by B'' with respect to B'. Assuming that the UV flux exponentially decays with the thickness x ($I^{\rm UV}(x) = I_0^{\rm UV}\ {\rm e}^{-\alpha x}$) the absorption coefficient α was computed. In the case of methanol we have photolysed five samples, each 1000 Å thicker than the previous one, in order to verify that the UV flux exponentially decays with the thickness.

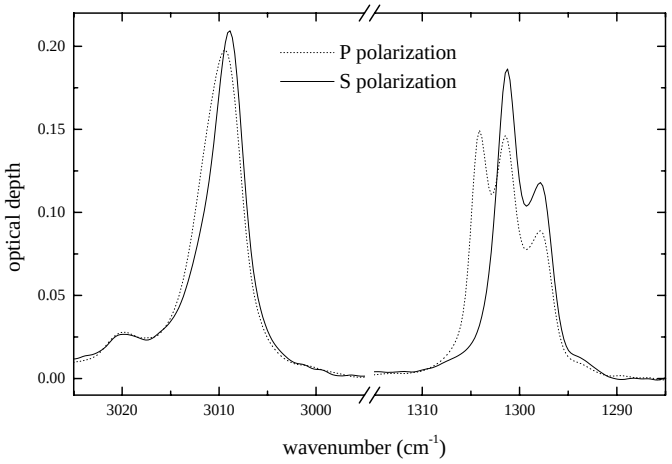

Fig. 3. Infrared absorption spectra of CH_4 at 12.5 K in the region of the C-H stretching and deformation modes taken in P (dotted line) and S (solid line) polarizations.

Using the method described above we have estimated the absorption coefficient of Lyman-α photons in CH_4, CH_3OH and H_2O ices at 12.5 K. We have found that these value 19 μm^{-1}, 12 μm^{-1}, and 28 μm^{-1} respectively. This latter value is in agreement with the value of 26 μm^{-1} estimated using the optical constants given by Warren (1984) at wavelength of 1210 Å. However since the optical constants of the samples change during photolysis and because the absorption coefficient depends on the optical constants these values refer to fresh ices. In particular, we have measured that the absorption coefficient of the ice sample initially made of pure methane increases to 33 μm^{-1} after 2.5×10^{18} incident photons cm^{-2} (i.e. after the highest dose investigated). In the following section we present the results relative to CH_4 and CH_3OH, while the effects induced on amorphous and crystalline water ice by ion and UV photon irradiation will be presented in a forthcoming paper (Baratta & Leto in preparation).

4. Ion irradiation vs. UV photolysis

4.1. CH_4 ice

Figure 3 shows the absorption spectra, in optical depth scale, of pure CH_4 taken in P and S polarization in the range of the C-H stretching (3010 cm^{-1}) and deformation (1300 cm^{-1}) modes. As already discussed by Baratta & Palumbo (1998) and Baratta et al. (2000) the spectrum taken in P polarization shows additional features not due to absorption (k) but to the increased reflectivity corresponding to the region across the absorption band where $n < 1$. The difference between the spectra in P and S polarization depends on the n and k values of the ice, however for a given sample also depends on the thickness, being higher for thinner films. In the following, if the profiles of the absorption features in the two polarizations are different, column densities of each species have been deduced from spectra taken in S polarization. The results

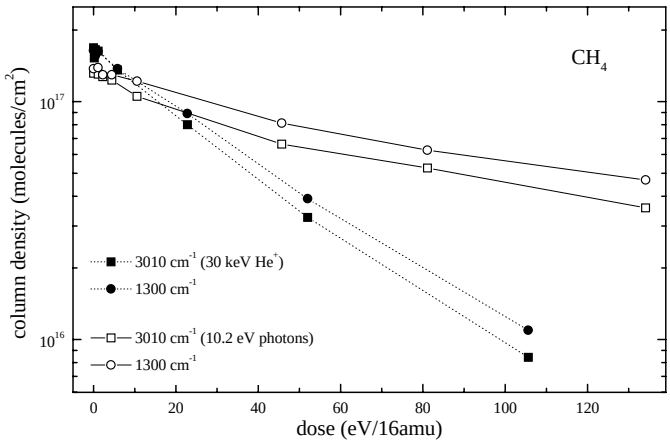

Fig. 4. Column density of CH_4 deduced from the C-H stretching (3010 cm^{-1}) and deformation (1300 cm^{-1}) modes after ion irradiation with 30 keV He^+ ions and photolysis with Lyman-α photons (10.2 eV). Solid and dotted lines have been drawn to guide the eye.

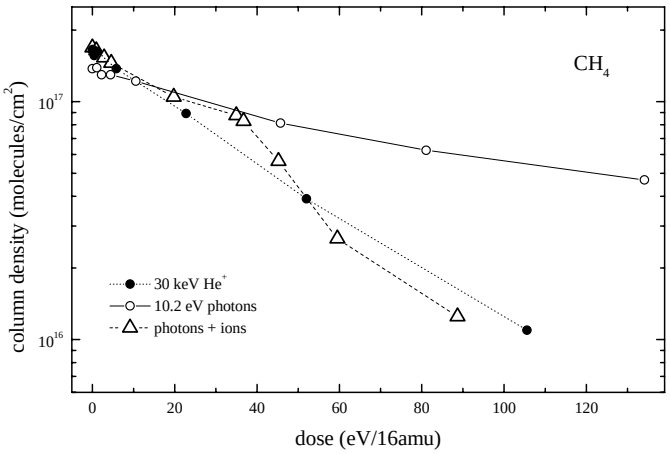

Fig. 5. Column density of CH_4 deduced from the 1300 cm^{-1} band (deformation mode) after ion irradiation with 30 keV He^+ ions (solid circles) and photolysis with Lyman-α photons (10.2 eV; open circles). Triangles refers to a sample which has been first processed with UV photons (up to 35 eV/16 amu) and then with He^+ ions. Straight lines have been drawn to guide the eye.

here presented do not change, as general trend, for unpolarized light. However, given that the absorption profiles and then the band area taken in unpolarized light do depend on the spectrometer response, which indeed is not the same in the two polarizations, the results obtained in S polarization can be better compared with those obtained in other experimental set-up.

Figure 4 shows the values of the column density of methane after ion irradiation with 30 keV He^+ and photolysis with Lyman-α photons at 12.5 K. In both cases the column density of the original sample is about 1.5×10^{17} molecules cm^{-2} (about 740 Å thick). In the case of ion irradiation the dose has been calculated from the knowledge of the stopping power (4×10^{-14} eV cm^2 $molecule^{-1}$) and of the integrated ion flux (ions cm^{-2}) which is directly related to the ion current measured during irradiation. In the case of UV photolysis the dose has been calculated from the knowledge of the integrated flux (photons cm^{-2}) of impinging photons measured by the wire detector during the experiment and of the percentage of impinging UV photons absorbed in the sample (estimated as described above).

It is evident that at the lowest doses ($\leq$20 eV/16 amu) the effects induced by UV photons and fast ions are comparable, that is the same number of CH_4 molecules are destroyed at the same doses. However as the dose increases the effects of photons and ions are different. In fact due to irradiation in both cases the optical constants of the sample change. It is well known that hydrocarbons evolve towards a polymer-like material and eventually to a refractory residue (Moore et al. 1983; Strazzulla et al. 1983; Strazzulla & Johnson 1991; Jenniskens et al. 1993). Also our experiments of UV photolysis show that a refractory residue is eventually formed. However while the energy released by ions is independent of the optical constants of the sample, the refractory residue is opaque to UV photons. Thus at higher doses impinging ions continue to release energy to the sample which is further modified while UV photons are strongly absorbed at increasing smaller depths as photolysis proceeds and cause negligible additional modifications.

Figure 5 shows the result of a *combined processing* experiment. An icy sample of pure CH_4 (triangles in the figure) has been first processed with UV photons (up to 35 eV/16 amu) and then with 30 keV He^+ ions (from 37 eV/16 amu to 89 eV/16 amu). In the same figure the results of ion irradiation and UV photolysis of pure methane are reported for comparison. These results strongly support the conclusions drawn above. In fact if a sample previously photolysed is ion irradiated a steep decrease (at the beginning even steeper than the case of ion irradiation alone) of CH_4 column density is observed.

In Fig. 4 column density of methane deduced both from the 3010 cm^{-1} and 1300 cm^{-1} bands are reported using A values 9.5×10^{-18} cm $molecule^{-1}$ and 6.4×10^{-18} cm $molecule^{-1}$ (Mulas et al. 1998) respectively. As expected after deposition the column density deduced from the two bands is the same and this is still true after ion irradiation and UV photolysis at the lowest doses. However as the dose increases the column density of methane deduced from the C-H stretching mode (3010 cm^{-1}) is always lower than the value deduced from the deformation mode (1300 cm^{-1}). This probably indicates that integrated absorption coefficients of pure ices are no longer appropriate after processing. Similar results were obtained after ion irradiation of methanol (Palumbo et al. 1999). In fact it has been shown that after ion irradiation the column density of methanol deduced from the 1460 cm^{-1} band is always larger than that deduced from the 1030 and 2830 cm^{-1} bands.

Figure 6 shows the column density of ethane (C_2H_6) and propane (C_3H_8) formed, along with other species, after ion irradiation and UV photolysis of pure methane at 12.5 K. Column density of ethane has been deduced from

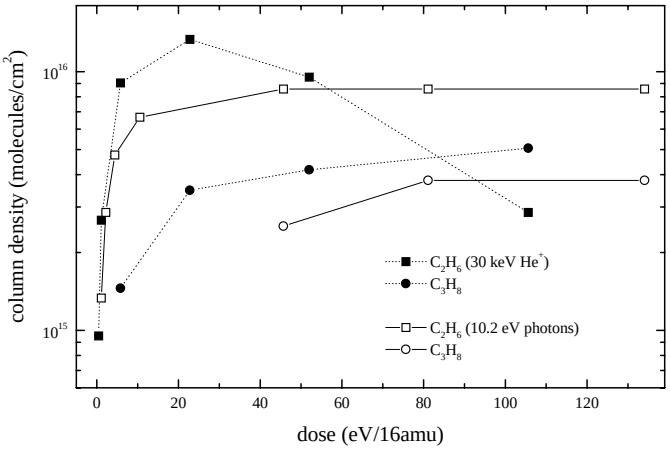

Fig. 6. Column density of C_2H_6 deduced from the 2976 cm^{-1} band and C_3H_8 deduced from the 2962 cm^{-1} band formed after ion irradiation with 30 keV He^+ ions and photolysis with Lyman-α photons (10.2 eV) of pure CH_4 at 12.5 K. Solid and dotted lines have been drawn to guide the eye.

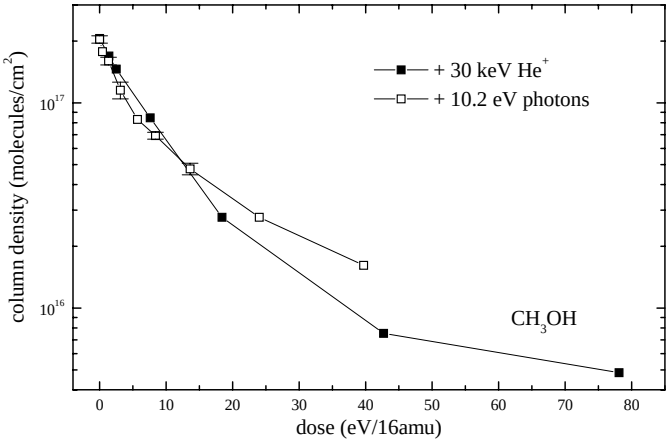

Fig. 7. Column density of CH_3OH, deduced form the 1026 cm^{-1} band, after ion irradiation with 30 keV He^+ ions and photolysis with Lyman-α photons (10.2 eV) at 12.5 K. Solid lines have been drawn to guide the eye.

the 2976 cm^{-1} band using $A = 1.05\times10^{-17}$ cm molecule^{-1} (Moore & Hudson 1998) and the column density of propane from the 2962 cm^{-1} band using $A = 1.58 \times 10^{-17}$ cm molecule^{-1} (Moore & Hudson 1998). At the lowest doses the trend of the column density of ethane is the same in the two experiments indicating that C_2H_6 is easily formed both after ion irradiation and UV photolysis of methane. However, after ion irradiation, as the dose increases, the column density of ethane reaches a maximum value and then decreases suggesting that after further irradiation ethane is destroyed and new species and eventually a refractory residue are formed. After UV photolysis the trend is different. In fact as the optical constants of the ice are modified by incoming photons, further photons are strongly absorbed at the surface of the sample and hence deeper layers are no longer affected by impinging photons. As a consequence, the column density of ethane remains almost constant after a dose of about 20 eV/16 amu.

4.2. CH_3OH ice

Figure 7 shows a comparison of the effects of ion irradiation and UV photolysis of pure CH_3OH at 12.5 K. In both cases the column density of the initial sample was about 2×10^{17} molecules cm^{-2} (about 1000 Å thick). The abundance of methanol has been deduced from the 1026 cm^{-1} band using $A = 1.3 \times 10^{-17}$ cm molecule^{-1} (Palumbo et al. 1999). Data points and errorbars relative to photolysis have been obtained from three separate equal experiments. Doses after ion irradiation have been estimated using a value of the stopping power equal to 5.4×10^{-14} eV cm^2 molecule^{-1}. Similarly to the case of CH_4, discussed above, at the lowest doses the trend of the column density is the same in the two experiments while differences exist at the highest doses.

Figure 8 shows the column density of CO and CO_2 formed after ion irradiation with 30 keV He^+ and UV Lyman-α photons of pure CH_3OH at 12.5 K. Column

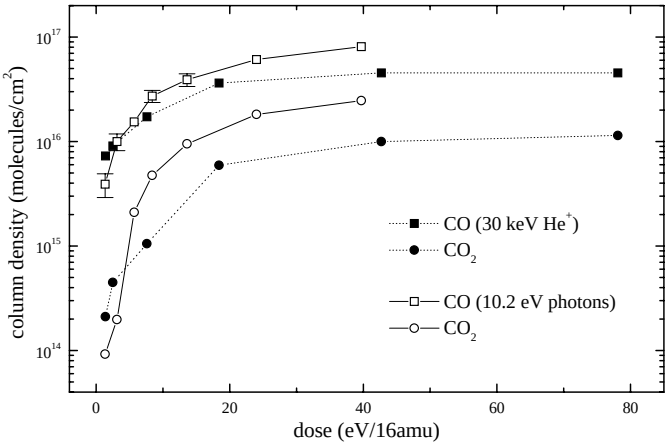

Fig. 8. Column density of CO deduced from the 2140 cm^{-1} band and CO_2 deduced from the 2340 cm^{-1} band formed after ion irradiation and UV photolysis of methanol at 12.5 K. Solid and dotted lines have been drawn to guide the eye.

density of CO has been deduced from the 2140 cm^{-1} band using $A = 1.1 \times 10^{-17}$ cm molecule^{-1} (Jiang et al. 1975) and column density of CO_2 from the 2340 cm^{-1} band using $A = 7.6 \times 10^{-17}$ cm molecule^{-1} (Yamada & Person 1964).

Figure 9 shows the column density of CH_4 and H_2CO formed after processing of pure CH_3OH at 12.5 K. Column density of methane has been deduced from the 1300 cm^{-1} band ($A = 6.4\times10^{-18}$ cm molecule^{-1}) and column density of formaldeyde from the 1720 cm^{-1} band using $A = 9.6 \times 10^{-18}$ cm molecule^{-1} (Schutte et al. 1993).

Figures 8 and 9 clearly show that starting from the same amount of methanol, a higher abundance of carbon dioxide and methane is formed after UV photolysis than after ion irradiation. This is in agreement with other results which indicate that one of the main effects of ion irradiation is the carbonization of the sample, that is preferential loss of hydrogen, oxygen, and nitrogen (Foti et al. 1991; Strazzulla & Baratta 1992).

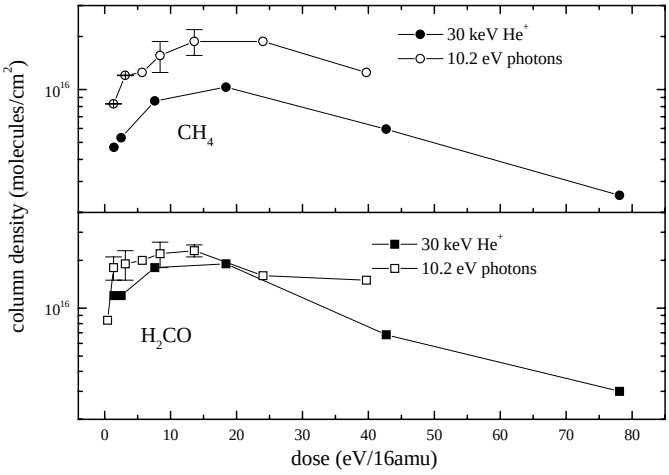

Fig. 9. Column density of CH_4 deduced from the 1300 cm^{-1} band and H_2CO deduced from the 1720 cm^{-1} band formed after ion irradiation and UV photolysis of methanol at 12.5 K. Solid lines have been drawn to guide the eye.

Finally, it could be argued that the differences found in the column densities after ion irradiation and UV photolysis of CH_4 and CH_3OH could be due to differences in the optical constants of the samples after different processing. We have verified that the band profiles from which column densities are deduced do not depend on the type of processing. Then we are confident that, as stated above, the differences found depend on the different interaction of ions and photons with matter.

5. Conclusion

Here we have presented the results of the comparison of the effects due to ion irradiation and UV photolysis of CH_4 and CH_3OH ices at 12.5 K. We have shown that at the lowest doses the effects induced by ions and UV photons are very similar while at higher doses some differences occur. In fact both processes modify the optical properties of the icy samples. However, while ions release energy to the sample independently of its optical properties, the interaction of UV photons with matter strongly depends on its optical properties. Thus the effects of ion irradiation and UV photolysis are comparable on fresh ices (i.e. at the lowest doses) while are very different as soon as the original ice sample is modified by the processing itself (i.e. at the highest doses).

Ices in space (on interstellar grains, planetary surfaces, comets) are continuously exposed to energetic processing by cosmic rays and UV photons. According to Moore (1999), icy grain mantles in dense molecular clouds absorb up to a few hundreds eV $molecule^{-1}$ due to cosmic ray and UV photon irradiation. These values includes the doses investigated in this work. However, as we have here shown, laboratory experiments are necessary to know whether the same amount of absorbed energy causes the same effects. On the other hand processing of icy surfaces in the Solar System and of cometary ices is dominated by energetic ions due to the low penetration depth of UV photons (∼200 Å) compared to that of ions (up to several cm for cosmic-ray protons).

It could be argued that icy grain mantles rich of CH_4 and CH_3OH may not be common in dense molecular clouds. However, regions rich of CH_4 may exist on planetary bodies (e.g., Douté et al. 1999). In any case the results here presented can be regarded as a first step in the study of the comparison of ion irradiation and UV photolysis of molecular ices.

Finally, Figs. 4 to 8 show that column densities of the original species in the icy sample and of newly formed species are not a linear function of the dose both after ion irradiation and UV photolysis. Hence the values of the formation and destruction rates (known as G values, i.e. the number of molecules produced by an absorbed energy of 100 eV), usually estimated at the lowest doses, cannot be estrapolated at higher doses and cannot be used to predict the composition of the ice mixture after any dose.

Acknowledgements. We would like to thank an anonymous referee for his critical reading of the paper and for his suggestion to perform the "combined processing" experiment which has given further support to our conclusions. We are grateful to F. Spinella for his valuable support in the laboratory. This research has been financially supported by the Italian Ministero dell'Università e della Ricerca Scientifica e Tecnologica (MURST).

References

Allamandola, L. J., Sandford, S. A., & Valero, G. J. 1988, Icarus, 76, 225
Baratta, G. A., & Palumbo, M. E. 1998, JOSA A, 15, 3076
Baratta, G. A., Leto, G., Spinella, F., Strazzulla, G., & Foti, G. 1991, A&A, 252, 421
Baratta, G. A., Palumbo, M. E., & Strazzulla, G. 2000, A&A, 357, 1045
Brown, W. L., Lanzerotti, L. J., & Johnson, R. E. 1982, Science, 218, 525
Cottin, H., Szopa, C., & Moore, M. H. 2001, ApJ, 561, L139
Douté, S., Schmitt, B., Quirico, E., et al. 1999, Icarus, 142, 421
Foti, A. M., Baratta, G. A., Leto, G., & Strazzulla, G. 1991, Europhys. Lett., 16, 201
Gerakines, P. A., Schutte, W. A., & Ehrenfreund, P. 1996, A&A, 312, 289
Gerakines, P. A., Moore, M. H., & Hudson, R. L. 2000, A&A, 357, 793
Groth, W. 1937, Z. Phys. Chem., 37, 307
Hagen, W., Allamandola, L. J., & Greenberg, J. M. 1979, Ap&SS, 65, 215
Jenniskens, P., Baratta, G. A., Kouchi, A., et al. 1993, A&A, 273, 583
Jiang, G. P., Person, W. B., & Brown, K. G. 1975, J. Chem. Phys., 64, 1201
Moore, M. H. 1999, Solid Interstellar Matter: the ISO Revolution, ed. L. d'Hendecourt, C. Joblin, & A. Jones (Springer-Verlag, New York), 199
Moore, M. H., & Hudson, R. L. 1992, ApJ, 401, 353
Moore, M. H., & Hudson, R. L. 1998, Icarus, 135, 518

Moore, M. H., Donn, B., Khanna, R., & A'Hearn, M. F. 1983, Icarus, 54, 388
Moore, M. H., Hudson, R. L., & Gerakines, P. A. 2001, Spectrochim. Acta A, 57, 843
Mulas, G., Baratta, G. A., Palumbo, M. E., & Strazzulla, G. 1998, A&A, 333, 1025
Palumbo, M. E., Castorina, A. C., & Strazzulla, G. 1999, A&A, 342, 551
Schutte, W. A., Allamandola, L. J., & Sandford, S. A. 1993, Icarus, 104, 118
Smith, M. A. H., Rinsland, C. P., Fridovich, B., & Rao, K. N. 1985, Molecular Spectroscopy: Modern Research, vol. III, ed. K. N. Rao (Academic Press, London), 111
Strazzulla, G., & Baratta, G. A. 1992, A&A, 266, 434
Strazzulla, G., & Johnson, R. E. 1991, in Comets in the Post-Halley Era, ed. R. Newburg Jr., M. Neugebaur, & J. Rahe (Kluwer, Dordrecht), 243
Strazzulla, G., Calcagno, L., & Foti, G. 1983, MNRAS, 204, 59
Strazzulla, G., Baratta, G. A., & Palumbo, M. E. 2001, Spectrochim. Acta A, 57, 825
Warren, S. G. 1984, App. Opt., 23, 1206
Westley, M. S., Baragiola, R. A., Johnson, R. E., & Baratta, G. A. 1995, Nature, 373, 405
Yamada, H., & Person, W. B. 1964, J. Chem. Phys., 41, 2478